Turkish Journal of Engineering

Turkish Journal of Engineering (TUJE)
Vol. 3, Issue 2, pp. 51-59, April 2019
ISSN 2587-1366, Turkey
DOI: 10.31127/tuje.433072
Research Article

INVESTIGATION OF MACHINABILITY PROPERTIES OF LASER TREATED S355JR CARBON STEEL WITH ZRB_2 NANOPARTICLES

Tuncay Şimşek [*1], Mustafa Bariş [2], Şadan Özcan [3,4] and Adnan Akkurt [5]

[1] Mersin University, Architecture Faculty, Department of Industrial Design, Mersin, Turkey
ORCID ID 0000-0002-4683-0152
tuncaysimsek@mersin.edu.tr

[2] Eti Maden Works General Management, Ankara 06010, Turkey
ORCID ID 0000-0002-2119-0697
mustafabaris@etimaden.gov.tr

[3] Hacettepe University, Faculty of Engineering, Department of Physical Engineering, Ankara, Turkey
[4] Hacettepe University, Division of Nanotechnology and Nanomedicine, Ankara,Turkey
ORCID ID 0000-0001-7966-1845
sadan@hacettepe.edu.tr

[5] Gazi University, Industrial Design Engineering, Ankara, Turkey
ORCID ID 0000-0002-0622-1352
aakurt@gazi.edu.tr

* Corresponding Author
Received: 11/06/2018 Accepted: 13/08/2018

ABSTRACT
In this study, the machinability properties of laser treated S355JR samples were investigated. The ZrB_2 nanoparticles were coated on the surface of S355JR carbon steel by 2 kW CO_2 laser. Then the coated samples were cut using the methods of abrasive water jet, wire-cut electrical discharge machining, laser, and abrasive disc, respectively. The phase structures and morphologies of the coated and cut surfaces were determined by using X-Ray diffractometry, optical microscope and scanning electron microscopy. The hardness was specified by using the microhardness device. It was found that low heat input and minimal damage was observed with the abrasive disc cutting method. Cutting with wire-cut electrical discharge machining, the worn zone was in a very narrow range, but there was also some heat-affected zone. While no heat input was seen in the method of cutting with abrasive water jet, significant damages in the shear edges and peripheral zones were observed due to abrasive particles. Intensive thermal deformation was also observed in the method of laser cutting.

Keywords: *Laser Coating, Nanoparticles, Machinability, Abrasive Water Jet, Wire-Cut Electrical Discharge Machining*

1. INTRODUCTION

Machining methods also develop as a result of developments in material technology. Machinability of new materials and traditional samples has been investigated for many years (Ozkul *et al.* 2013; Aouici *et al.,* 2014; Buldum *et al.,* 2012). Due to improperly selected methods, materials cannot fulfil their functions in critical processes and serious economic losses occur. Therefore, it is very important to determine the most appropriate cutting method for the produced materials. It is known that the high temperature materials such as TiC (Wang *et al.*, 2013), B_4C (Yibas *et al.*, 2015), WC (Pulsford *et al.,* 2018), SiC (Hashemi *et al.,* 2018), TiN (Zhang *et al.,* 2017), Al_2O_3 (Ruppi,, 2005), ZrC (Zhang *et al.,* 2018), TiB_2 (Han et al., 2018) etc. are coated on the base materials such as carbon and cold work steel (Pei *et al.,* 1996; Suresh *et al.,* 2018; (Sun et al., 2018), aluminum (Chi *et al.,* 2018), magnesium (Xu *et al.,* 2014), titanium alloys etc (Zhao *et al.,* 2018). The methods, such as self-propagating high temperature synthesis (SHS) (Masanta *et al.,* 2010), thermal spray coatings (Berger *et al.*, 2015), sol-gel (Tlili *et al.*, 2016), PVD (Lu *et al.,* 2018), and CVD (Liu *et al.,* 2018), reactive plasma spraying (Dai et al., 2017), are used intensively for coating of metals. Being one of these high temperature ceramics, zirconium diboride (ZrB_2) which has a melting temperature of 3245 ^oC, high hardness, oxidation resistance and thermal shock resistance, are mostly used in a wide area as diffusion barriers in the semiconductors, molten metal container, and ignition absorber in nuclear reactor cores (Fahrenholtz *et al.,* 2007; Sonber *et al.,* 2011; Baudis *et al.*, 1985). ZrB_2 nanoparticles can be obtained by using many different methods. Peters *et al*. (2009), obtained single phase ZrB_2 by grinding elemental Zr, and B powders in a Spex type high energy ball mill. Akgün *et al.* (2011), produced ZrB_2 using ZrO_2, Mg and B_2O_3 powders through mechanochemical method and volume combustion synthesis method. Setoudah *et al.* (2006), milled an elemental mixture of ZrO_2, B_2O_3 and Mg by using a laboratory scale mill under Ar atmosphere and synthesized a pure ZrB_2 with approximately 75 nm crystallite. Jalaly *et al*. (2013), obtained nanocrystal ZrB_2 from ZrO_2, B_2O_3 by magnesiothermic and aluminothermic reductions. Guo *et al.* (2009), produced ZrB_2 powders in the vacuum by boron/carbothermal reduction of ZrO_2, B_4C, and C. It is also seen that ZrB_2 significantly increases the wear and corrosion resistance when it coated on the material surfaces (Xue *et al.,* 2018; Zou *et al.,* 2017; Neuman *et al.*, 2017; Cheng *et al.,* 2017; Dangio *et al.,* 2018; Pourasad *et al.,* 2017).

Parts used in industries such as machine, manufacturing, space and automotive etc. deteriorate after a certain performance and mandatory changes in geometries are required. In the case of replacing high-cost parts with new ones, it is more economical to make some modification to these parts instead of replacing them. While, there are many studies about different coating metals such as steel, carbon steel, aluminum, copper, titanium alloys etc. in the literature, no study has been found especially about machinability of these coated materials. The properties of coated samples was lack to date. Considering this gap in literature, the S355JR carbon steel materials coated with ZrB_2 nanoparticles are subjected to micro cutting with widely used methods such as abrasive water jet, wire-cut electrical discharge machining, laser and abrasive disc cutting methods, respectively. Experimental studies have been focused on determination of how the coating layer is affected by these processes than the cut surface. In the present study, the mechanochemical synthesis method was preferred as the synthesis method because of the advantages such as occurrence of the reaction at room temperature, being an economical method, great flexibility in the selection of the processing parameters, ability to produce large quantities of material with the same physical properties and offering the possibility of producing compounds which cannot be produced by using conventional methods (Avar *et al.*, 2015; Simsek *et al.*, 2017). Synthesized ZrB_2 nanoparticles are coated with CO_2 laser after determining the optimum parameters on the surface of S355JR (St52) carbon steel materials. Besides its wide usage area in many fields such as aviation, automotive and manufacturing industries, its poor wear properties were effective in the selection of the base material. As coating method, laser coating method is chosen due to its important advantages which allows to obtain hard, protective, abrasion and corrosion resistant coating on the surfaces of metals. By utilizing superior properties of the laser beam; hard, homogenous, non-porous, crack-free coatings with high wear resistance can be obtained on the surfaces by melting a thin layer on the substrates surface. The ideal cutting (machining) method for samples coated with ZrB_2 nanoparticles was investigated in detail. The cut samples were examined by using optical and SEM microscopy and X-Ray diffractometry without any treatment. Hardness of coated and cut surfaces were determined.

2. EXPERIMENTAL STUDIES

2.1. Materials

Mechanochemically synthesized ZrB_2 nanoparticles were used as the coating material. ZrB_2 nanoparticles were obtained by milling Zr (873.05 μm, ≥ 99, Sigma Aldrich), Mg (138.66 μm, ≥99.00%, Sigma Aldrich), and B_2O_3 (545.74 μm, ≥98.00%, Eti Maden) under Ar atmosphere in a high energy ball mill (Fritch, P6) for 30h. The powder mixture consisting of MgO and ZrB_2 phases after 30h ball milling was purified with acetic acid (AA, CH_3COOH) solution, dried under vacuum, and then used in the coating applications. The detailed synthesis procedures of ZrB_2 nanoparticles are presented in (Simsek 2014).

2.2. Laser Coating and Machinability Experiments

S355JR carbon steel was used as the substrate material in the coating experiments. Table 1 shows the chemical composition of S355JR carbon steel.

Table 1. Chemical composition of S355JR carbon steel

Chemical Composition (wt %)	C	Si	Mn	P	S	Cu	N	Fe
	0.22	0.55	1.60	0.035	0.035	0.55	0.09	Bal.

The size of the base material used was 100 (length) X 15 (width) X 4 (thickness) mm. Prior to laser cladding, the samples were sandblasted and cleaned with acetone and ethanol. Firstly, the nanoparticles were coated on the surface of carbon steel with a thickness of 50 µm and all precoating processes were carried out in the vacuum. Then, the layers were heated up to 400 oC under Ar atmosphere for 4 hours to make good bond to substrate and convert the phenolic resin to carbon (Yilbas et al., 2011). This carbon film provides hard wear resistant carbide phases on the surface. This process was done very carefully because if the precoating was not done well, some problems was encountered such as adhesion to the substrate, inhomogeneity and porosity (Yilbas et al., 2012; Simsek et al., 2017). Secondly, the precoated layers were laser clad by a 2 kW CO2 laser (Amada, LC-2415 α III, Japan) at continuous-wave mode under N_2 gas atmosphere. Table 2 shows the laser coating parameters.

Table 2. Laser coating parameters

Laser power	W	2000
Power density	W/mm^2	181
Frequency	Hz	1000
Scanning rate	mm/s	5
Average power	W	160
Laser wave length	Mm	10.64
N_2 pressure	kPa	600

Fig. 1. shows the schematic view of laser cladding process and nozzle used. The coating experiments were conducted between 75-200 W laser powers under N_2 atmosphere. It is noticed that the higher and lower laser power usage resulted in very intensive cracks and pores. Due to obtaining homogenous distribution of nanoparticles without fractures and cracks, the samples of 160 W of laser power was used in the machinability experiments.

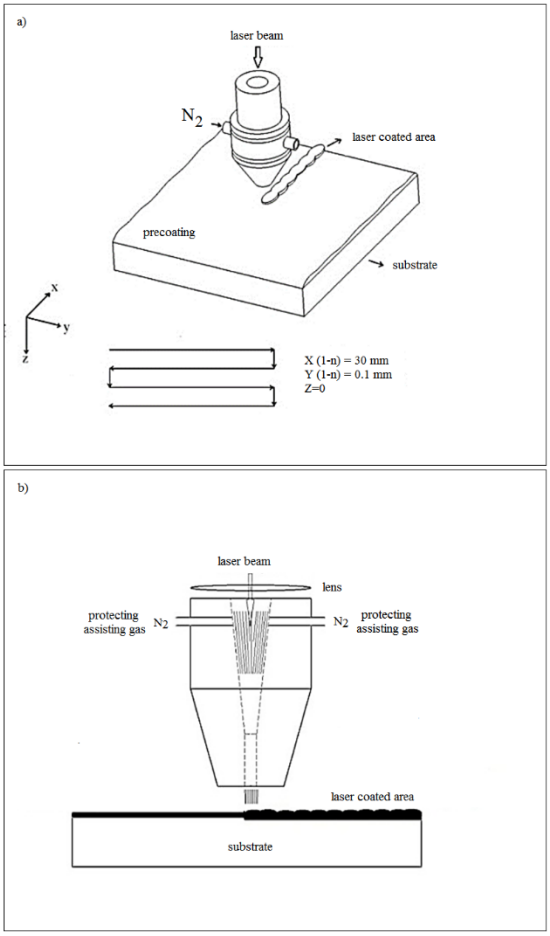

Fig. 1. Schematic view of a) laser coating process b) nozzle (Simsek 2014).

Machinability properties of the samples in respect of cutting methods were determined by cut with abrasive water jet (KMT, SLV-E50), wire-cut electrical discharge machining (Makino, Dou 43), laser (Amada, Lasmac LC-2415 α III), and abrasive disk (BMS, Bulucut-3), respectively. Table 3 shows the applied cutting parameters.

Table 3. Parameters applied in cutting tests

Abrasive water jet cutting		*Laser cutting*	
Nozzle Diameter	0.75 mm	Laser Power	2000 W
Sand Flow Rate	250 g/min	Cutting Speed	1000 mm/min
Pressure	4000 bar	Frequency	1000 Hz
Feed rate	150 mm/min	Duty	55 %
		Average Power	880 W
Wire-cut electrical discharge machining		*Abrasive disc cutting*	
Wire Diameter	0.3 mm	Disc Used	SiC
Wire Type	CuZn	Disc Sizes	250x32x1.6 mm
Wire Speed	6 m/min	Revolutions Speed	2840 rpm
Cutting Speed	11 mm/min	Feed rate	1 mm/s
Tension	10 cN	Cutting System	Automatic
Time of Energy Given	18 ms	Cooling	Cooling with fluid
Time of Energy Cut	70 ms		

2.3. Characterization

The phase structures of the coating layers were determined by XRD (Rigaku D/MAX-2200) with CuKα (λ=1.5408 °A) radiation by selecting 40 kV operating voltage and 30 mA current, 2θ angle range 2-90°, and 4°/min scanning rate. The average crystallite size of the nanoparticles were calculated with Scherrer Equations [Eq.1], where τ is the crystallite size, K is the constant taken depending on the shape of crystal (0.89), λ is the wavelength of X ray (0.154 nm), β is the width of half-length of peak (FWHM), and θ is Bragg angle. In the calculation of crystallite size, FWHM values of (100) peak in XRD patterns were determined by graphic analysis using JADE 7.0 XRD analysis program.

$$\tau = \frac{K \,.\, \lambda}{B \,.\, Cos\,\theta} \qquad (1)$$

Microstructural examinations of the surface and cross-sections of the samples were characterized by scanning electron microscope (FEI Quanta 200F) and optical microscope (Leica M205 C). The hardness of samples was determined by using a Vickers hardness tester (Shimadzu HMV-2) under 50 g load for 15 s.

.

3. RESULTS AND DISCUSSION

As coating material ZrB_2 nano particles were used. XRD graphs of synthesized and purified nanoparticles are given in Fig. 2. The crystallite size of the purified nanoparticles was calculated as 20.45 nm by Scherrer formula. The powder mixtures of MgO and ZrB_2 were purified with hot acetic acid leaching and following to purification processes, ZrB_2 nanoparticles were carefully precoated on carbon steel and coated with a CO2 laser at 160 W laser power (Simsek 2014).

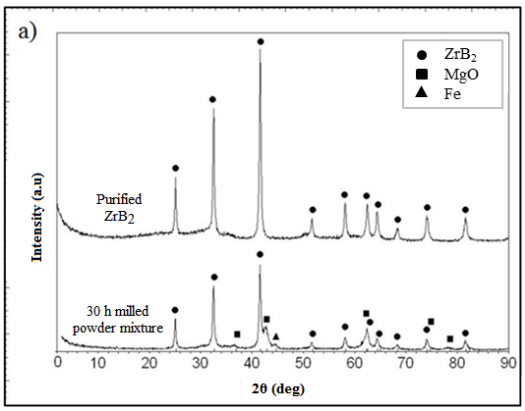

Fig. 2. XRD graph of the ZrB_2 nanoparticles (Simsek 2014).

Fig. 3. shows the SEM and optic images of the coated sample surfaces and the cross-sections. Homogeneous, nonporous and crack-free layers with good metallurgical bonding to substrate can be seen from Fig. 3. The thickness of layers was around 24 µm while the heat affected zone was around 60 µm

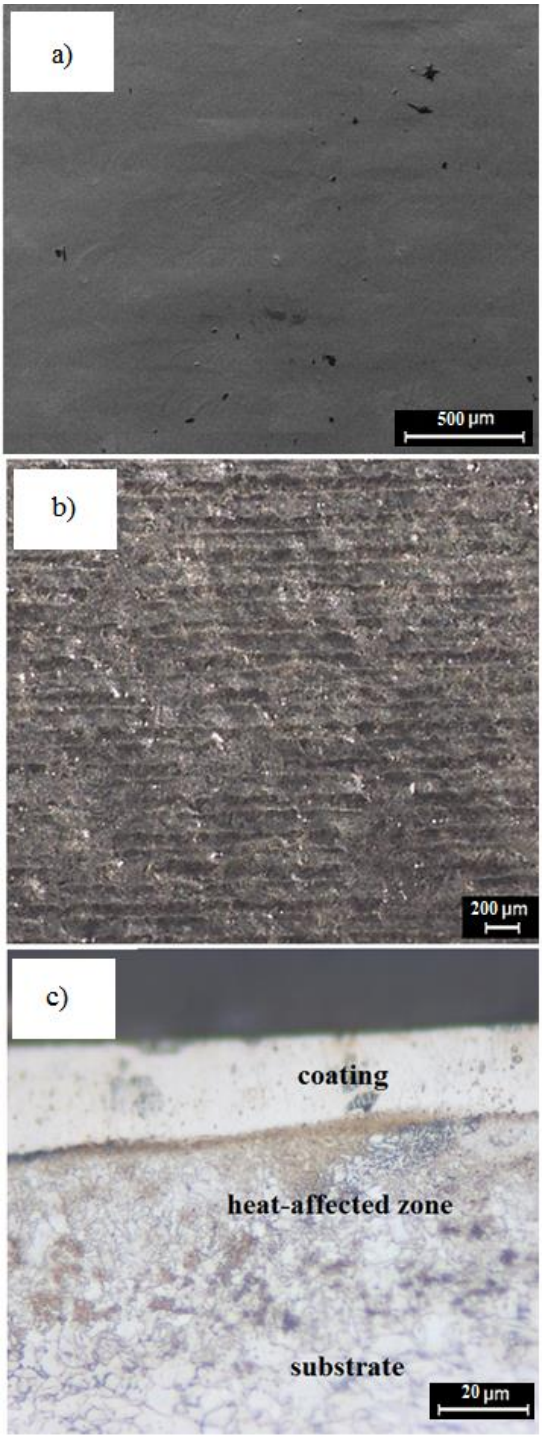

Fig. 3. a) Surface view (SEM), b) Surface view (optical microscope), c) Cross-section view (optical microscope) (Simsek 2014).

The phase structures were identified by X-Ray diffractometry. Fig. 4a shows the XRD analysis and hardness profiles of the coating layers obtained at 160 W laser power (Simsek 2014, Simsek 2017). $ZrN_{0.4}B_{0.6}$, Fe_3C and $FeN_{0.0760}$ $Zr_7O_8N_4$ phases were observed on the surfaces of the coating layers. Nitride phases were formed with the reaction of assisting–protecting N_2 gas at high temperatures while the carbide phase occurred with the reaction of carbon film formed on the substrate (Fig. 4a).

The same results were also observed by Yilbas et al. studies. They reported in their laser cladding experiments that N_2 gas resulted to formation of nitride phases on the substrate (Yilbas et al, 2012). Microhardness tests were performed for determining the hardness of the coating surface. Fig. 4b. represents the average hardness value of 5 measurements were taken from the every region of coating layers. It can be seen from Fig. 4b. that the hardness was about 220 HV, 600 HV, and 900 HV for substrate, heat–affected zone and coatings layers, respectively. It is noticed that the formation of Fe, Zr-rich carbide, boride and nitride phases substantially increased the coating layers hardness.

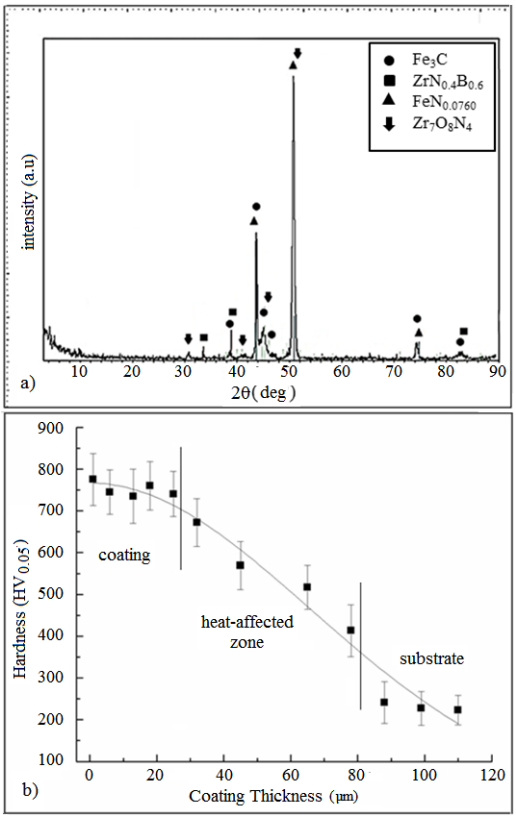

Fig. 4. a) XRD pattern of coating, b) Regional cross-section hardness values of the coated samples

Furthermore, in order to examine the regional structure properties of the coating layer, the heat-affected zone and base metal, the coated sample was left in liquid nitrogen for 10 minutes and then broken. Fig. 5. shows SEM images of the cross-sections of the fracture samples. When the images were examined, it was determined that a transition region was formed between the coating layer and the heat-affected zone, the structures of coating layer (a), heat-affected zone (b) and base metal (c) were different from each other due to the applied high heat. As a result of the high temperature releasing during the laser coating, columnar structures were observed in the hardened coating layer due to the rapid cooling; whereas, brittle ruptures in the coating layer and ductile fractures from transition region to the base metal after the fracture were observed (Simsek 2014).

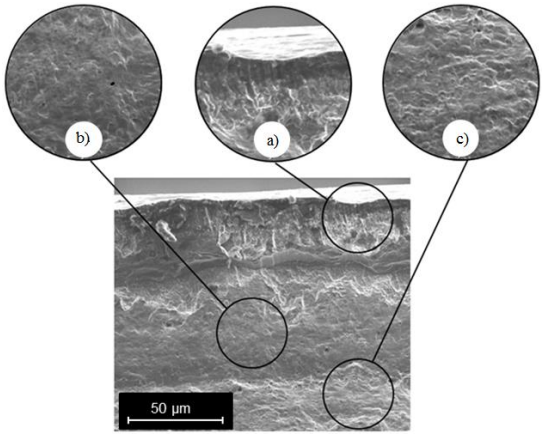

Fig. 5. SEM image of the structures released a result of the fracture of the coated samples in liquid nitrogen

After microstructural analysis of coated layer, the machinability performance of coated S355JR carbon steel layers were investigated with cutting the layers by advanced manufacturing methods such as abrasive water jet, wire-cut electrical discharge machining, laser and abrasive disc. Fig. 6. and 7 shows the optical microscope and SEM images of the samples cut with abrasive water jet, wire–cut electrical discharge machining, laser and abrasive disc, respectively. The cut samples were examined carefully and the deformations made by the methods on the coating layers were determined. When the optical microscope and SEM images of the cutting regions of S355JR carbon steel surface were evaluated; destructions of ~200 μm in cutting with abrasive water jet, ~150 μm in cutting with laser beam, ~25 μm in cutting with wire-cut electrical discharge machining and ~10 μm in cutting with abrasive disc were observed (Simsek, 2014). It is known that cutting process can be achieved with high pressure hydro-abrasive jet in water–jet system. Firstly, the pump generates a flow of pressurized water and granular abrasive is drawn into the water stream. In order to form and stabilize, the mixture of water and abrasive particles passes through the nozzle and directed to the surface of materials. With stream of this high pressure hydro–abrasive jet toughest materials can be cut successfully. The quality of cut layers are depending on the machining parameters such as water pressure, traverse speed, abrasive flow rate, and standoff distance etc. (Kumar et al., 2017; Uthayakumar et al., 2016; Hajdarevic et al., 2015). The parameters of cutting is given in Table 3. Jet-splashes are inevitable in the abrasive water jet cutting process (including uncoated specimens) by the use of thin water jets under high pressure with added abrasive slurry. These jet-splashes are scattered on the surface of the jet hit, backwards or backwards at a certain angle. Because of this situation, the coating layer has deformed significantly. At the cut surfaces, it was found that the roughness of the surface increased in the cutting area, and large peaks and valleys was appeared on the surfaces (Fig. 7a.) It was also observed that all the samples obtained had significant damage in the shear edges and peripheral zones of coating layer and the abrasive particles in the mixed state with water were buried from the coating layer to the next transition zone even in far distances. This is an expected situation, so it has been determined that cutting of

nanoparticle coated materials with an abrasive water jet will not be an appropriate choice. The surface of samples cut with laser was significantly affected by the heat. The irregularity in the coating thickness on the shear edge surface increased compared to other cutting methods and a certain amount of loss (along with the evaporation and molten sub-metal) was observed from the coating material. Surface cracks are also another major problem due to high heat input and sudden cooling during cutting of the samples with laser. In addition, it has been found that the formation of droplet due to melting of main material and coating material causes a substantial damages of the cut surface geometry (Bouzakis et al., 2017; Siebert et al., 2014). It has been determined that laser cutting should not be preferred in the processing of the surfaces coated with nanoparticles, even though its use in micro processing methods is getting widespread every day. However, when the obtained data's were evaluated, it is a more acceptable method than the abrasive water jet.

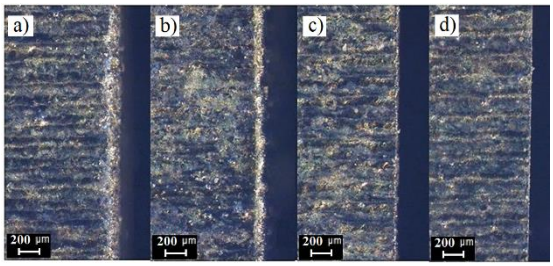

Fig. 6. Optical microscope (X100) images of the ZrB_2 coated samples after cutting processes; a) Abrasive water jet, b) Laser, c) Wire–cut electrical discharge machining, d) Abrasive disc

When the cut zones of samples obtained through wire-cut electrical discharge machining method were examined, it was observed that the coating, transition zone and substrate were affected by heat in a more limited way but there were even small amounts of residues (burr) on the cutting surface (Puri et al., 2005; Hascalik et al., 2004). By usage of cutting fluid in the process of cutting with abrasive disc, the heat effect was minimized when compared to wire-cut electrical discharge machining and smother shear edge was obtained.

The microhardness of cut layers are given in Fig. 8. Microhardness measurement of the cross-section of the cut samples were carried out after sample preparation procedures like polishing and etching. As a result of the sample preparation procedures, it was observed that the destruction zones caused by the cutting methods were eroded, so that the measurements were taken from the inner regions of the samples and it is observed that the microhardness values were very close to each other (Fig. 8). While damage occurred in laser and wire–cut electrical discharge machining cutting among thermal cutting methods due to heat, the effect of abrasive grains and the pressurized water was in question in abrasive water jet. Although there was no damage in cutting with abrasive water jet due to heat, abrasive grains deformed the cutting zone severely as a result of their random scatterings on the coating surface. The results showed that the method of cutting with abrasive disc was the most suitable cutting method in the positions where the machining capability is suitable but the wire-cut electrical discharge machining method should be preferred in the complicated geometric samples for which abrasive disc could not be used.

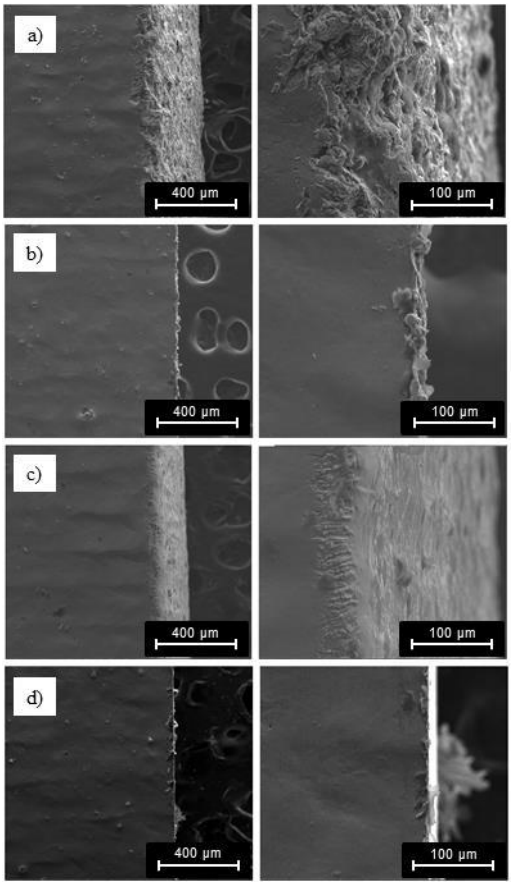

Fig. 7. SEM (X800) images of ZrB_2 coated samples after the cutting process; a) Laser beam b) Abrasive water jet, c) Wire – cut electrical discharge machining, d) Abrasive disc

When an overall evaluation was made, it was observed that processes of cutting with laser beam (due to thermal effect) and abrasive water jet (due to the impact of abrasive particles having random distribution in water) caused severe destruction on the coating layer. However, a small amount of damage was determined due to the thermal effect in method of cutting with wire-cut electrical discharge machining. It was found that minimum damage was seen in process of cutting with abrasive disc. Structural deformations were observed in a wide region due to heat dissipation as well as thin cracks and fractures on the surface caused by sudden high heat input and sudden cooling in the process of cutting with laser. In the method of cutting with wire-cut electrical discharge machining, there were smaller cracks and fractures related to heat on the surface. In addition, a much smaller region was affected by heat compared to the laser, and consequently structural deformations remained limited. There was no thermal deformation in the method of cutting with abrasive water jet since there was no heat input but as a result of were observed on the coating surface with the abrasive particle penetration. Cutting with abrasive random splashes of water-abrasive mixture

on the surface at the beginning of the cutting process, significant ruptures on the coating surface and great amount of physical deformations disc was determined as the most efficient method among these methods.

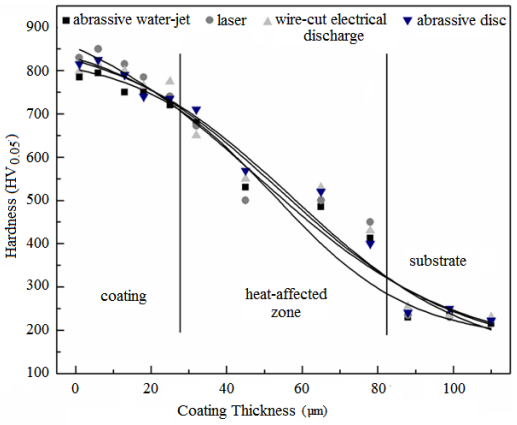

Fig. 8. Comparison of regional hardness values of ZrB_2 coated samples after cutting processes depending on the cutting method

4. CONCLUSIONS

The machinability of ZrB_2 nanoparticles coated S355JR carbon steel layers were investigated in the present study. 2 kW CO_2 laser with 2000 W power was operated at continuouswave mode was used for the laser coating applications. The layers without cracks and porosity obtained with 160 W laser power were used as specimen for cutting operations. The laser coated layers were cut with abrasive water jet cutting, wire-cut electrical discharge machining, laser and abrasive disc, respectively. The microstructural, morphological and phase structures were determined by using optic microscopy, scanning electron microscopy and X-Ray diffractometry. The findings are,

- When the coating area was evaluated in respect of machinability applications, minimal damage and the best surface properties were achieved in the method of cutting with abrasive disc.
- It was determined that abrasive water jet cutting should not be used for nanoparticle coated surfaces unless it is necessary. Random splashes of water-abrasive mixture on the surface at the beginning of the cutting process, significant ruptures on the coating surface and great amount of physical deformations occur on the coated layers surfaces. When the damage on the cutting surface was evaluated, it was determined that the method causing maximum damage in the coating layer was the abrasive water jet.
- Laser cutting method is also not suitable for cutting of this kind of coatings, due to a certain amount of loss (along with the evaporation and molten sub-metal) from the coating material and surface cracks due to high heat input and sudden cooling during cutting of the samples. In addition, it has been also seen that the formation of droplet due to melting of main material and coating material causes a substantial damages of the cut surface geometry.
- When the cut zones of samples obtained through wire-cut electrical discharge machining method were examined, it was observed that the coating, transition zone and substrate were affected by heat in a more limited way but there were even small amounts of residues (burr) on the cutting surface. Beyond its disadvantages, it is seen that thermal methods like laser and wire-cut electrical discharge machining, also minimize the rupture tendency of the coating from the substrate
- In the process of cutting with abrasive disc, by usage of cutting fluid the heat effect was minimized and smother shear edge was obtained.
- Microstructural investigations of the cutting regions of S355JR carbon steel surface were revealed the destructions of ~200 µm in cutting with abrasive water jet, ~150 µm in cutting with laser, ~25 µm in cutting with wire-cut electrical discharge machining and ~10 µm in cutting with abrasive disc.
- It was seen that cutting methods generally did not cause a significant change in hardness of cut layers, but even with small differences, the highest hardness occurred in the cutting made by laser beam and the lowest hardness occurred in the cutting with abrasive water jet. The hardness of cut layers were varied in the range of 780-865 HV.

ACKNOWLEDGEMENTS

The authors would like to thank Development of Technology Department, Eti Maden Works General Management for laboratory facilities.

REFERENCES

Akgün, B., Çamurlu, H.E., Topkaya, Y., Sevinç, N. (2011). "Mechanochemical and volume combustion sythesis of ZrB_2." *International Journal of Refractory Metals and Hard Materials*, Vol. 29, pp. 601-607

Aouici, H., Bouchelaghem, H. Yallese, M. A., Elbah, M., Fnides, B. (2014) " Machinability investigation in hard turning of AISI D3 cold work steel with ceramic tool using response surface methodology." *International Journal of Advanced Manufacturing Technology*, Vol.73, pp. 1775–1788.

Avar, B., Ozcan, Ş. (2015). "Characterization and amorphous phase formation of mechanically alloyed Co60Fe5Ni5Ti25B5 powders." *Journal of Alloys and Compounds* Vol. 650, pp. 53-58.

Baudis, U., Fitchte, R. (1985). Boric oxide and boric acid and borates, Schwetz, KA, Lipp A, Capbll FT, Pfefferkom R(Eds.). Boron carbide, boron nitride, and metal borides, Zirconium and zirconium compounds, Ullmann's Encyclopedia of Industrial Chemistry, Fifth, Completely Revised Edition A4, Wiley-VCH, Weinheim, 263-307, 91.

Berger, L.M. (2015). "Application of hardmetals as thermal spray coatings." *International Journal of Refractory Metals and Hard Materials*, Vol. 49, pp. 350–364.

Buldum, B.B., Şık, A., Ozkul, I. (2012). "Investigation of Magnesium Alloys Machinability." *International Journal Of Electronics; Mechanical And Mechatronics Engineering,* Vol.2, pp. 261-268.

Bouzakis, K.D., Charalampous, P., Kotsanis, T., Skordaris, G., Bouzakis, E., Denkena, B., Breidenstein, B., Aurich, J.C., Zimmermann, M., Herrmann, T., M'saoubi R. (2017). "Effect of HM substrates' cutting edge roundness manufactured by laser machining and micro-blasting on the coated tools' cutting performance." *CIRP Journal of Manufacturing Science and Technology, Vol.* 18, pp. 188–197.

Cheng, E. J., Li., J., Sakamoto, Y.., Han, S., Sun, H., Noble, J., Katsui, H., Goto, T. (2017). "Mechanical properties of individual phases of ZrB_2-ZrC eutectic composite measured by nano indentation." *Journal of the European Ceramic Society,* Vol. 37, pp. 4223-4227.

Chi, Y., Gu, G., Yu, H., Chen, C. (2018). "Laser surface alloying on aluminum and its alloys: A review." *Optics and Lasers in Engineering,* Vol. 100, pp. 2337.

Dangio, A., Zoua, J., Binner, J., Ma, H.B., Hilmas, G.E., Fahrenholtz, W.G. (2018). "Mechanical properties and grain orientation evolution of zirconium diboride-zirconium carbide ceramics." *Journal of the European Ceramic Society,* Vol. 38, pp. 391-402.

Dai, X., Yan, D., Yang, Y., Chu, Z., Chen, X., Song, J. (2017). "In situ $(Al,Cr)_2O_3$-Cr composite coating fabricated by reactive plasma Spraying." *Ceramic International,* Vol. 43, pp. 6340-6344.

Fahrenholtz, W.G., Hilmas, G.E. (2007). "Refractory Diborides of Zirconium and Hafnium", *Journal of American Ceramic Society, Vol.* 90(5), pp. 1347-1364.

Hascalik, A., Caydas¸ A. (2004). "Experimental study of wire electrical discharge machining of AISI D5 tool steel." *Journal of Materials Processing Technology*, Vol. 148, pp. 362–367.

Hashemi, S.H., Shoja-Razavi, R. (2016). "Laser surface heat treatment of electroless Ni–P–SiC coating on Al356 alloy." *Optics and Laser Technology,* Vol. 85, pp. 1–6.

Han, Y.G., Yang, Y., Wang, L., Chen, X.G., Chu, Z.H., Zhang, X.N., Dong, Y.C., Liu, Z., Yan, D.R. Zhang, J.X., Li, C.G. (2018). "Microstructure and properties of in-situ TiB_2 matrix composite coatings prepared by plasma spraying." *Applied Surface Science,* Vol. 431, pp. 48-54.

Hajdarevic, D. B., Cekic, A., Mehmedovic, M., Djelmica, A. (2015). "Experimental Study on Surface Roughness in Abrasive Water Jet Cutting." *Procedia Engineering* Vol. 100, pp. 394 – 399.

Jalaly, M,, Bafghi, M.Sh., Tamizifar, M., Gotor, F.J. (2013). "Mechanosynthesis of nanocrystalline ZrB_2-based powders by mechanically induced self-sustaining reaction method." *Advanced in Applied Ceramics,* Vol. 112 (7), pp. 383-388.

Guo, W.M., Zhang, G.J. (2009). "Reaction Processes and Characterization of ZrB_2 Powder Prepared by Boro/Carbothermal Reduction of ZrO_2 in Vacuum." *Journal of the American Ceramic Society,* Vol. 92, pp. 264–267.

Kumar, A., Singh, H., Kumar, V. (2017). "Study the parametric effect of abrasive water jet machining on surface roughness of Inconel 718 using RSM-BBD techniques." *Materials and Manufacturing Processes*, pp. 1-7.

Liu, C., Liu, Z., Wang, B. (2018). "Modification of surface morphology to enhance tribological properties for CVD coated cutting tools through wet micro-blasting post-process." *Ceramic International,* Vol. 44, pp. 3430-3439.

Lu, C., Yao, J.W., Wang, Y.X., Zhu, Y.D., Guo, J.H., Wang, Y., Fu, H.Y., Chen, Z.B., Yan, M.F. (2018) "A novel anti-frictional multiphase layer produced by plasma nitriding of PVD titanium coated ZL205A aluminum alloy." *Applied Surface Science,* Vol. *431,* pp. 32-38.

Masanta, M., Ganesh. P., Kaul, R., Choudhury, A.R. (2010). "Microstructure and mechanical properties of TiB_2–TiC–Al_2O_3-SiC composite coatings developed by combined SHS, sol–gel and laser technology." *Surface and Coatings Technology,* Vol. 204, pp. 3471–3480.

Neuman, E.W., Hilmas, G.E., Fahrenholtz, W.G. (2017). "Processing, microstructure, and mechanical properties of zirconium diboride-boron carbide ceramics." *Ceramic International,* Vol. 43, pp. 6942-6948.

Ozkul, I., Buldum, B.B., Akkurt, A. (2013). "Machinabilty of Sleipner Cold Work Steel With Wire Electro Discharge Machining". *International Journal Of Electronics; Mechanical And Mechatronics Engineering,* Vol.2, pp. 252-260

Pulsford, J., Kamnis, S., Murray, J., Bai1, M., Hussain, T. (2018). "Effect of Particle and Carbide Grain Sizes on a HVOAF WC-Co-Cr Coating for the Future Application on Internal Surfaces: Microstructure and Wear." *Journal of Thermal Spray Technology,* Vol. 27, pp. 207–219.

Pei, Y.T., Ouyang, J.H, Lei, T.C. (1996). "Laser cladding of ZrO_2-(Ni alloy) composite coating." *Surface and Coatings Technology,* Vol. 81, pp. 131-135.

Peters, J.S., Cook, B.A., Harringa, I., Russell, A.M. (2009). "Erosion resistance of TiB_2-ZrB_2 composites." *Wear,* Vol. 267, pp. 136-143.

Pourasad, J., Ehsani, N. (2017). "In-situ synthesis of SiC-ZrB_2 coating by a novel pack cementation technique to protect graphite against oxidation." *Journal of Alloys and Compounds,* Vol. 690, pp. 692-698.

Puri, A.B., Bhattacharyya, B. (2005). "Modeling and analysis of white layer depth in a wire-cut EDM process through response surface methodology." *International Journal of Advanced Manufacturing Technology,* Vol.25, pp. 301–307.

Ruppi, S. (2005). "Deposition, microstructure and properties of texture-controlled CVD a-Al_2O_3 coatings." International *Journal of Refractory Metals and Hard Materials*, Vol. 23, pp. 306–316.

Siebert, R., Schneider, J., Beyer, E. (2014). "Laser Cutting and Mechanical Cutting of Electrical Steels and its Effect on the Magnetic Properties." *Ieee Transactions On Magnetics*, Vol. 50 (4), 2001904-2001908.

Suresh, S., Rangarajana, S., Bera, S., Krishnan, R., Amirthapandian, S., Sivakumar, M., Velmurugan, S. (2018). "Evaluation of corrosion resistance of nano nickel ferrite and magnetite double layer coatings on carbon steel." *Thin Solid Films*, Vol. 645, pp. 77-86.

Sun, C., Xue, Q., Zhang, J., Wan, S., Tieu, A.K., Tran, B.H. (2018). "Growth behavior and mechanical properties of Cr-V composite surface layer on AISI D3 steel by thermal reactive deposition." *Vacuum*, Vol. 148 pp. 158-167

Sonber, J.K., Suri, A.K. (2011). "Synthesis and Consolidation of Zirconium Diboride: Review." *Advances in Applied Ceramics, Vol.* 110 (6), pp. 321-334.

Setoudeh, N., Welham, N.J. (2006). "Formation of zirconium diboride (ZrB_2) by room temperature mechanochemical reaction between ZrO_2, B_2O_3 and Mg." *Journal of Alloys and Compounds*, Vol. 420, pp. 225-228.

Şimşek, T. (2014). Investigation of The Zirconium Diboride Nanocrystal Coated Different Materials Mechanic and Mechinability Properties. Ph. D. Thesis, University of Gazi, Ankara, Turkey.

Simsek, T., Baris, M., Chattoopahyay, A. K., Ozcan, S., Akkurt, A. (2017). Surface Treatment of S355JR Carbon Steel Surfaces with ZrB_2 Nanocrystals by CO_2 Laser." *Transactions of the Indian Institute of Metals*, Vol. 71, pp. 1885-1896.

Simsek, T., Baris, M., Kalkan, B. (2017). "Mechanochemical processing and microstructural characterization of pure Fe2B nanocrystals." *Advanced Powder Technology*, Vol. 28 (11), pp. 3056-3062.

Tlili, B., Barkaoui, A., Walock, M. (2016). "Tribology and wear resistance of the stainless steel. The sol–gel coating impact on the friction and damage." *Tribology International*, Vol. 102, pp. 348-354.

Uthayakumar, M., Khan, M.A., Kumaran, S.T., Slota, A., Zajac, J. (2016). "Machinability of Nickel-Based Super alloy by Abrasive Water Jet Machining." *Materials and Manufacturing Processes*, Vol. 31 (13), pp. 1733-1739.

Wang, X.H., Pan, X.N., Du, B.S., Li, S. (2013). "Production of in situ TiB2+TiC/Fe composite coating from precursor containing B4C-TiO2-Al powders by laser cladding." *Transactions of Nonferrous Metals Society of China*, Vol. 23, pp. 1689-1693.

Xu, J., Zou, B., Fan, X., Zhao, S., Hui, Y., Wang, Y., Zhou, X., Cai, X., Tao, S., Ma, H., Cao, X. (2014). "Reactive plasma spraying synthesis and characterization of TiB_2–TiC–Al_2O_3/Al composite coatings on a magnesium alloy." *Journal of Alloys and Compounds*, Vol. 596, pp. 10–18

Xue, C., Zhou, H., Hu, J., Wang, H., Xu, J., Dong, S. (2018) "Fabrication and microstructure of ZrB_2–ZrC–SiC coatings on C/C composites by reactive melt infiltration using ZrSi2 alloy." *Journal of* Advanced *Ceramics*, Vol. (7), pp. 64-71.

Yilbas, B.S., Karatas, C., Karakoc, H., AbdulAleem, B.J., Khan, S., Al-Aqeeli N. (2015). "Laser surface treatment of aluminum based composit mixed with B_4C particles." *Optics and Laser Technology*, Vol. 66, pp. 129–137.

Yilbas, B.S., Akhtar, S.S., Karatas, C. (2011). "Laser carbonitriding of alumina surface." *Optics and Lasers in Engineering, Vol.* 49, pp. 341–350.

Yilbas, B.S., Al-Aqeeli N, Karatas, C. (2012). "Laser control melting of alümina surfaces with presence of B_4C particles." *Journal of Alloys and Compounds*, Vol. 539, pp. 12-16.

Zhang, M., Araez, N.G. (2017). "A sol–gel route to titanium nitride conductive coatings on battery materials and performance of TiN-coated LiFePO4." *Journal of Materials Chemistry A*, Vol. 5, pp. 2251-2260.

Zhang, Y., Wang, H., Li, T., Fu, Y., Ren, J. (2018). "Ultra-high temperature ceramic coating for carbon/carbon composites against ablation above 2000 K." *Ceramic International*, Vol. 44, pp. 3056-3063.

Zhao, X., Zhang, P., Wang, X., Chen, Y., Liu, H., Chen, L., Sheng, Y., Li, W. 2018). "In-situ formation of textured TiN coatings on biomedical titanium alloy by laser irradiation." *Journal of the Mechanical Behavior of Biomedical Materials*, Vol. 78, pp. 143-153

Zou, J., Rubio, V., Binner, J. (2017). "Thermo ablative resistance of ZrB_2-SiC-WC ceramics at 2400 ^oC." *Acta Materialia, Vol.* 133, pp. 293-302.